Inclination-Driven Thin-Film Dynamics: Geometry-Induced 2 Regime Ordering in the (*Bo*, *Pe*, *Da*) Space

Helena Cristina Vasconcelos , Reşit Özmentes , Maria Meirelles *

Posted Date: 26 March 2026

doi: 10.20944/preprints202603.2106.v1

Keywords: thin liquid films; inclined surfaces; lubrication theory; interfacial hydrodynamics; gravitational symmetry breaking; dimensionless scaling; wet–dry intermittency; confined transport

 doi:10.20944/preprints202603.2106.v1

Article

Inclination-Driven Thin-Film Dynamics: Geometry-Induced Regime Ordering in the (*Bo*, *Pe*, *Da*) Space

Helena Cristina Vasconcelos [1,2], Reşit Özmenteş [3] and Maria Meirelles [1,4,*]

[1] Faculty of Science and Technology, University of the Azores, Ponta Delgada, S. Miguel, 9500-321 Azores, Portugal

[2] Laboratory of Instrumentation, Biomedical Engineering and Radiation Physics (LIBPhys, UNL), Department of Physics, NOVA School of Science and Technology, 2829-516 Caparica, Portugal

[3] Vocational School of Health Services, Bitlis Eren University, 13100 Bitlis, Türkiye

[4] Research Institute of Marine Sciences of the University of the Azores (OKEANOS), Horta, Faial, 9901-862 Azores, Portugal

* Correspondence: maria.gf.meirelles@uac.pt

Abstract

We develop a unified theoretical framework for thin-film hydrodynamics on inclined solid substrates, integrating capillarity, intermolecular forces, gravitational symmetry breaking, confined transport, and stochastic wetting into a single formulation. Starting from lubrication theory with capillary curvature and disjoining-pressure interactions, we obtain a general thin-film equation that incorporates inclination-driven advection, nanoscale stabilization, and humidity-controlled source–sink fluxes. A dimensionless analysis shows that, within the long-wave lubrication approximation, inclination induces a leading-order coupling among the Bond, Péclet, and Damköhler numbers. This coupling defines a characteristic inclination-parameterized trajectory $\Gamma(\theta)$ in the (Bo, Pe, Da) space: material parameters set the system's position along this curve, while the geometric constraint governs the ordering of hydrodynamic, transport, and confinement regimes. We further derive quantitative crossover criteria associated with transport transitions ($Pe \simeq 1$) and reactive-confinement loss ($Da \simeq 1$), providing explicit regime boundaries that can be evaluated for representative parameter ranges. A representative parameterization of an ultrathin atmospheric electrolyte film is then used to make these crossovers explicit, yielding illustrative inclination thresholds for the onset of transport reorganization and reactive-confinement loss. Coupling the deterministic structure to a minimal stochastic closure captures intermittent wet–dry dynamics under environmental forcing. In this closure, inclination selectively accelerates the drying pathway through the drainage time (and thus λ_{dry}), while re-wetting remains primarily humidity-controlled, providing a leading-order basis for wet-state persistence and time-of-wetness versus θ. The resulting framework provides a general physical description of confined films under geometric asymmetry, relevant to wetting, interfacial drainage, confined transport, and thin-film systems in which symmetry breaking and coupled interfacial–transport processes coexist across scales.

Keywords: thin liquid films; inclined surfaces; lubrication theory; interfacial hydrodynamics; gravitational symmetry breaking; dimensionless scaling; wet–dry intermittency; confined transport

1. Introduction

Thin liquid films on solid surfaces constitute a canonical setting for studying the interplay between geometry, intermolecular forces and hydrodynamics. Their behavior governs wetting, adhesion, drainage, lubrication, interfacial transport and rupture, and has long served as a testbed for theories of capillarity, surface forces and thin-film flow [1–3]. When the film thickness reaches micro- and nanometric scales, the balance between capillary curvature, van der Waals interactions

 doi:10.20944/preprints202603.2106.v1

and viscous dissipation becomes highly sensitive to perturbations. Even weak geometric asymmetries can reorganize drainage pathways, stability criteria and rupture dynamics [4–6].

Among such asymmetries, inclination plays a distinctive physical role. Rather than acting as a minor geometric detail, inclination introduces a symmetry-breaking field that couples directly to the drainage flux through the tangential gravitational forcing $\rho g \sin\theta$. Classical analyses typically treat thin films in horizontal or weakly perturbed geometries [3,7,8], but natural and technological interfaces—ranging from atmospheric electrolyte layers to evaporating or deliquescent coatings—rarely remain horizontal. Such films undergo cycles of thinning, rupture, re-wetting and coalescence under the combined action of gravity, capillarity and disjoining pressure [7–10].

Experimental observations and modeling studies indicate that inclination strongly affects wet-film behavior: inclined surfaces tend to display faster thinning, earlier rupture, and shorter wet-state persistence than horizontal substrates [11,12]. Related thin-film regimes also arise in lubrication systems [10], soft-matter and colloidal films [13], confined interfacial transport [14], evaporating and deliquescent layers, and thin-film flows governed by competing advection–diffusion mechanisms [15,16]. Despite this diversity, many treatments analyze capillarity, disjoining pressure, gravitational drainage, confined electrostatics and stochastic wetting separately, without explicitly clarifying how geometric asymmetry reorganizes these mechanisms in a coordinated way.

A central difficulty is that inclination simultaneously re-weights transport, stability and confinement: it strengthens tangential drainage (via Bo), shifts the advection–diffusion hierarchy (via Pe), and modifies reactive accessibility under confinement (via Da). Although these dimensionless groups are often treated as independently adjustable control parameters, their dependence on film thickness and drainage implies that they are not fully independent under inclination. Here we show that, at leading order within lubrication theory, inclination does not explore the full {Bo, Pe, Da} parameter space but instead constrains the dynamics to a geometry-imposed, one-parameter trajectory $\Gamma(\theta)$. This reduction provides a useful organizing structure for identifying regime ordering and crossover conditions without scanning the entire parameter space.

We develop a unified theoretical framework that consolidates these mechanisms within a single continuum formulation. Starting from lubrication theory with capillary curvature and disjoining-pressure interactions, we derive the governing thin-film equation in a form that makes inclination-driven advection, nanoscale stabilization and humidity-controlled source–sink fluxes explicit. A central outcome of the analysis is that inclination induces a coordinated, leading-order coupling of the Bond, Péclet and Damköhler numbers inherited directly from the structure of the lubrication flux. Therefore, the system evolves along a one-parameter path $\Gamma(\theta)$ in (Bo, Pe, Da) space, providing a systematic basis for analyzing stability, drainage, confined transport and reactive accessibility under geometric asymmetry.

The main physical consequences are:

(i) Inclination enforces a coordinated re-weighting of the control groups such that (Bo, Pe, Da) evolve along a single geometry-imposed path $\Gamma(\theta)$ rather than varying independently.

(ii) This re-weighting produces an ordered sequence of transport and confinement crossovers (Pe $\simeq$ 1; Da $\simeq$ 1) that can be evaluated directly from material and environmental parameters.

(iii) The same structure provides closure to a minimal stochastic wet–dry model by linking the drying rate λ_{dry} to the deterministic drainage time, thereby yielding explicit trends for wet-state persistence and time-of-wetness as functions of θ.

Beyond conceptual unification, the formulation yields quantitative regime criteria. In particular, the inclination-driven scaling of Pe and Da provides explicit crossover conditions separating diffusion-dominated, mixed and advection-dominated transport, as well as the progressive loss of reactive confinement as Da decreases. We then couple the deterministic thinning dynamics to a minimal stochastic wet–dry model, in which inclination selectively accelerates the drying pathway via the drainage time while leaving re-wetting largely humidity-controlled. This deterministic–stochastic coupling provides explicit scaling relations for wet-state persistence without introducing chemistry-specific assumptions.

 doi:10.20944/preprints202603.2106.v1

The resulting formulation is general at the level of continuum thin-film hydrodynamics and provides a surface-physics framework for understanding geometric asymmetry in confined films across hydrodynamics, interfacial physics and soft-matter systems. While the present work emphasizes analytical structure and scaling, the governing equations also provide a direct basis for targeted asymptotic or numerical analyses in specific material contexts.

2. Governing Equations and Coupled Film Dynamics

Thin-film dynamics on an inclined solid substrate arise from the coupled action of viscous flow, capillary curvature, intermolecular forces, gravitational symmetry breaking and humidity-controlled source–sink fluxes. This section derives the governing equations from lubrication theory and establishes the structure required for the dimensionless analysis in Section 3.

2.1. Lubrication Framework and Gravitational Symmetry Breaking

Consider a liquid film of local thickness $h(x,t)$ on a substrate inclined at an angle θ. Under the long-wave approximation $h/L \ll 1$ and $|\partial_x h| \ll 1$, the lateral flow is well described by lubrication theory. A schematic of the inclined thin-film geometry and the relevant forces is shown in Figure 1.

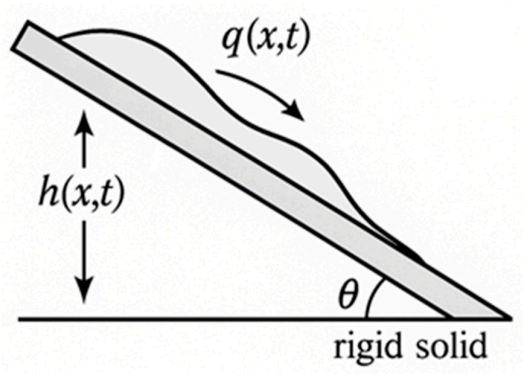

Figure 1. Schematic representation of a thin liquid film on an inclined solid substrate.

The depth-averaged volumetric flux per unit width, denoted $q(x,t)$, is [3,4]:

$$q(x,t) = -\frac{h^3}{3\mu}\,\partial_x(\gamma\,\partial_{xx}h + \Pi(h)) + \frac{\rho g \sin\theta}{3\mu}\,h^3 \quad (1)$$

where

- μ is viscosity,
- γ is surface tension,
- $\Pi(h)$ is the disjoining pressure,
- $\rho g \sin\theta$ is the tangential gravitational forcing.

Mass conservation then gives:

$$\partial_t h + \partial_x q = S(x,t), \quad (2)$$

with $S(x,t)$ representing condensation–evaporation fluxes. Inclination enters solely through the $\sin\theta$ term, acting as a symmetry-breaking field that biases drainage without altering capillary or intermolecular contributions. This formulation applies broadly to ultrathin films dominated by viscous, capillary and van der Waals forces [1,2,5].

This structure also makes clear that inclination enters the governing flux only through gravitational contribution, which becomes the leading-order source of θ-dependence in the dimensionless groups derived in Section 3.

The thin-film flux in Eq. (1) is derived under the standard lubrication assumptions of Newtonian viscosity, no-slip at the solid surface, small interfacial slopes $|\partial_x h| \ll 1$, negligible inertia ($Re \ll 1$), and a separation of scales $h/L \ll 1$. Slip, if present, modifies only the mobility prefactor $h^3/3\mu$ and

 doi:10.20944/preprints202603.2106.v1

does not alter the leading-order structure of the capillary, disjoining-pressure or gravitational terms. The formulation is not intended to describe molecularly thin precursor layers or regimes in which continuum hydrodynamics, the disjoining-pressure model, or the classical mobility law break down. Within these constraints, Eq. (1) captures the dominant balance of forces governing micrometric and nanometric films on inclined substrates and provides the appropriate starting point for the nondimensional analysis of Section 3.

From Eq. (1), a characteristic downslope velocity scale follows immediately from the gravitational mobility,

$$U_\theta \sim \frac{\rho g H^2}{3\mu} \sin\,\theta, \quad (3)$$

and the corresponding drainage time scale is $T_\theta \sim L/U_\theta$. These two quantities provide direct quantitative access to inclination-controlled regime boundaries used later: $Pe(\theta) \sim U_\theta L/D$ and $Da(\theta) \sim kH/U_\theta$. Thus, even before full numerical integration, the governing structure yields measurable inclination-dependent crossover criteria.

2.2. Capillary Curvature and Intermolecular Forces

Capillary pressure is

$$P_c = -\gamma\ \partial_{xx} h, \quad (4)$$

which stabilizes short-wavelength disturbances. Intermolecular forces enter through the disjoining pressure [2]:

$$\Pi(h) = -\frac{A}{6\pi h^3} + \Pi_{\mathrm{rep}}(h), \quad (5)$$

with A the Hamaker constant and $\Pi_{\mathrm{rep}}(h)$ representing electrostatic or structural repulsion [6,17].

Related disjoining-pressure models for both volatile and nonvolatile thin films, including dry-spot growth and film-disappearance scenarios, are discussed in [18].

Absent gravity, the competition between P_c and $\Pi(h)$ yields the classical spinodal-dewetting instability [7,9].

Inclination does not modify $\Pi(h)$ or capillarity itself; instead, it accelerates access to the ultrathin regime where $\Pi'(h)$ controls stability, thereby shortening rupture times and biasing instability pathways downslope through the gravitational flux [3,4].

2.3. Source–Sink Terms and Environmental Coupling

Humidity-driven processes enter through

$$S = S_{\mathrm{cond}}(RH, T) - S_{\mathrm{evap}}(T, h), \quad (6)$$

describing condensation/deliquescence and evaporation [19,20].

These fluxes control re-wetting cycles, rupture recovery and wet/dry intermittency— behaviors characteristic of humidity-driven electrolyte films on exposed surfaces [11,12].

2.4. Confined Electrostatics in Ultrathin Films

For electrolyte films, the electric potential $\phi(x,t)$ satisfies

$$\nabla \cdot [\kappa(h) \nabla \phi] = 0, \quad (7)$$

where $\kappa(h)$ is the thickness-dependent conductivity, reduced in nanometric films by electrical double-layer overlap [2].

Boundary conditions:

- solid–liquid interface: $-\kappa\, \partial_n \phi = j_{\mathrm{int}}$
- liquid–air interface: $\partial_n \phi = 0$

Electric relaxation is much faster than hydrodynamic dynamics [14], justifying the quasi-static approximation.

2.5. Ionic Advection–Diffusion and Reactive Transport

The solute concentration satisfies

$$\partial_t c + \partial_x (uc) = D\ \partial_{xx} c + R(c, h, \phi), \quad (8)$$

 doi:10.20944/preprints202603.2106.v1

where

- $u = q/h$ is the depth-averaged lateral velocity,
- D is the diffusivity,
- R represents reactive or electrochemical processes.

Inclination modifies solute retention through the ratio uL/D, linking gravitational drainage to mass-transport resistance and reactive confinement [15,16].

2.6. Structure of the Coupled Thin-Film Fields

The coupled fields

$$\{h(x,t),\ c(x,t),\ \phi(x,t)\} \quad (9)$$

provide a complete continuum-scale description of the dynamics of inclined thin films. Within the lubrication framework, these equations capture the leading-order balance among viscous flow, capillarity, intermolecular forces, gravitational forcing and confined transport.

This formulation is valid under the usual long-wave assumptions: small interfacial slopes, negligible inertia, Newtonian viscosity and film thicknesses sufficiently large for continuum hydrodynamics to apply. Molecularly thin precursor layers, strong-slip conditions and Knudsen-scale effects lie outside the range of applicability of this leading-order model.

The nondimensional structure emerging from these equations is developed in Section 3.

3. Dimensionless Formulation and the Inclination-Driven Trajectory

The dimensionless structure of the governing equations reveals how inclination reshapes the relative contributions of capillarity, intermolecular forces, gravitational drainage and confined transport. When expressed using appropriate characteristic scales, the thin-film equations reduce to a compact form governed by three natural dimensionless groups: the Bond, Péclet and Damköhler numbers.

The coordinated dependence of these groups on the inclination angle defines a leading-order trajectory in the (Bo, Pe, Da) parameter space. This geometry-imposed trajectory constrains the behavior of all inclined thin-film systems, setting the structure developed in the subsections below.

3.1. Characteristic Scales and Nondimensional Variables

A natural starting point for the nondimensional analysis is to identify the characteristic scales that describe the geometry and dynamics of the inclined film. Let H denote a representative film thickness, L a lateral length scale, U the drainage velocity associated with gravitational forcing, and $T = L/U$ the corresponding advective timescale. Because of the gravitational contribution to the lubrication flux scales as $\rho g h^3 \sin\theta$, the velocity scale U is chosen to preserve this leading-order dependence on θ, ensuring that inclination appears explicitly—and solely—through gravity-driven advection in the dimensionless formulation.

Using these scales, the dimensional variables are expressed in nondimensional form as

$$x = Lx', h = Hh', t = Tt', q = UH\,q', \quad (10)$$

where primes are omitted after substitution.

With these definitions, the mass-conservation law becomes

$$\partial_t h + \partial_x q = \mathrm{Da}_0 S * (RH, T, h), \quad (11)$$

where Da_0 is a nondimensional source–sink strength and $S^*(RH, T, h)$ is an $\mathcal{O}(1)$ dimensionless source–sink function representing the humidity-controlled balance of condensation/deliquescence and evaporation (cf. Section 2.3).

The corresponding nondimensional flux takes the form

$$q = -h^3[\mathrm{Ca}^{-1}\ \partial_{xxx} h - \partial_x \Pi^*(h) - \mathrm{Bo}\sin\theta], \quad (12)$$

with

$$\mathrm{Ca} = \frac{\mu U}{\gamma}, \mathrm{Bo} = \frac{\rho g H L}{\gamma},\ \Pi^*(h) = \frac{H}{\gamma}\,\Pi(h). \quad (13)$$

 doi:10.20944/preprints202603.2106.v1

Here $Bo = \rho g H L/\gamma$ is the Bond number based on the film thickness H and the lateral scale L used in the lubrication scaling.

In this representation, inclination enters only through $\mathrm{Bo}\sin\theta$, isolating the geometric contribution to the force balance independently of the specific material parameters.

This nondimensionalization makes explicit that inclination enters the system only through the gravitational mobility and therefore drives correlated changes in all dimensionless groups. As a result, variations in θ cannot be interpreted independently in terms of hydrodynamics, transport or reaction, but necessarily move the system along a single constrained path in parameter space.

3.2. Balance Between Capillarity, Intermolecular Forces and Gravity

The nondimensional flux highlights the competing roles of capillary curvature, intermolecular forces and gravitational drainage in determining thin-film dynamics.

In nondimensional form, these contributions scale as

- $\mathrm{Ca}^{-1}\ \partial_{xxx}h$ (capillarity),
- $-\partial_x \Pi^*(h)$ (intermolecular forces),
- $-\mathrm{Bo}\sin\theta$ (gravity),

while viscous resistance enters through the geometric factor h^3.

Because these terms enter additively into the flux, inclination modifies the relative magnitude of the competing contributions rather than their absolute scale. As θ increases, the gravitational term grows through $\mathrm{Bo}\sin\theta$, while the capillary and intermolecular terms remain unchanged. This introduces a progressive reweighting of the force balance:

- the gravitational contribution strengthens monotonically,
- the effective stabilizing influence of capillarity weakens in relative terms,
- the film becomes increasingly sensitive to intermolecular attraction at small thickness.

The inclination angle θ therefore acts as a natural organising parameter for dynamics, altering the hierarchy of competing forces without affecting the structure of the governing equations. The crossover $Bo \sim 1$ therefore defines a measurable inclination-dependent transition between capillary-stabilised and gravity-dominated film morphologies.

3.3. Solute Transport and the Péclet Number

Solute transport in the draining film is governed by the interplay between advection, diffusion and reaction. In nondimensional form, the transport equation reads

$$\partial_t c + \partial_x(uc) = \mathrm{Pe}^{-1}\ \partial_{xx}c + R(c,h,\phi), \quad (14)$$

where the dimensionless velocity is $u = q/h$ and the Péclet number

$$\mathrm{Pe} = \frac{UL}{D} \quad (15)$$

measures the relative strength of advective drainage to diffusive redistribution.

Because the characteristic velocity U arises from the gravitational component of the lubrication flux (Section 2.1), it increases monotonically with inclination. Consequently,

$$\mathrm{Pe}(\theta) \propto \sin\ \theta, \quad (16)$$

implying that inclination drives the system across three distinct transport regimes:

- Diffusion-dominated regime ($\mathrm{Pe} \ll 1$):
  concentration gradients relax efficiently, and transport is primarily controlled by confinement through $h(x,t)$.
- Intermediate regime ($\mathrm{Pe} \sim 1$):
  advection and diffusion compete, generating longitudinal concentration gradients and coupling transport to film morphology.
- Advection-dominated regime ($\mathrm{Pe} \gg 1$):
  solutes are rapidly displaced downslope, residence times shorten, and the system becomes sensitive to even small variations in inclination.

These regimes arise directly from the nondimensional structure of the governing equations and reflect the geometric amplification of transport associated with increasing θ. The condition $Pe(\theta) \approx$

 doi:10.20944/preprints202603.2106.v1

1 marks the transition from solute retention to advective flushing, providing a direct criterion for when inclined films cease to accumulate dissolved species.

3.4. Reactive Confinement and the Damköhler Number

Reactive processes within the film introduce an additional nondimensional parameter, the Damköhler number, which compares the timescale of reaction to the timescale of advective transport. For a reaction rate k, the nondimensional form is

$$\mathrm{Da} = \frac{kL}{U}. \quad (17)$$

Because the drainage velocity U is set by gravitational forcing and increases monotonically with the inclination angle θ, the Damköhler number decreases accordingly:

$$\mathrm{Da}(\theta) \propto \frac{1}{\sin\theta}. \quad (18)$$

This inverse dependence has direct implications for reactive confinement:

- Reaction-dominated regime ($\mathrm{Da} \gg 1$):
  solute residence times exceed reactive timescales; reactivity is governed primarily by film thickness and intermolecular interactions.
- Transport-limited regime ($\mathrm{Da} \ll 1$):
  advection removes solute faster than it can react; reaction becomes constrained by supply rather than kinetics.
- Coupled regime ($\mathrm{Da} \sim 1$):
  comparable timescales lead to strong sensitivity to local variations in $h(x,t)$, $u(x,t)$ and confined electrostatics.

The inclination-controlled shift from reaction-dominated to transport-dominated behavior is therefore an intrinsic feature of inclined thin-film systems, arising directly from the nondimensional structure of the governing equations. It also underpins the shortening of reactive intervals and the reduction of wet-state persistence analyzed in Section 4.

The inclination-driven decrease of $Da(\theta)$ implies that increasing θ shifts the system from reaction-dominated to transport-limited behavior, even when intrinsic kinetics remain unchanged.

3.5. Inclination-Driven Trends in $\{Bo, Pe, Da\}$ Space

The nondimensional structure derived in Sections 3.1–3.4 reveals a coordinated dependence of the Bond, Péclet and Damköhler numbers on the inclination angle. To leading order,

$$Bo \propto sin\theta, Pe \propto sin\theta, Da \propto (sin\theta)^{-1},$$

so that a change in θmodifies the three dimensionless groups in a fully coupled manner.

These relations follow directly from the nondimensional lubrication flux (Section 3.1), in which gravitational forcing contributes solely through the term $Bo\ \sin\theta$, while the velocity scale U inherits the same θ-dependence.

Under the assumptions of the long-wave lubrication approximation (Newtonian viscosity, no slip at the substrate, $h/L \ll 1$, negligible inertia, and source–sink terms that do not introduce additional intrinsic length or velocity scales), this coordinated dependence defines a geometry-imposed, leading-order trajectory $\Gamma(\theta)$ in the $\{Bo, Pe, Da\}$ space. Figure 2 summarizes this structure: (a) shows the projection of $\Gamma(\theta)$ onto the (Bo, Pe) plane, (b) shows the associated $Da(\theta)$ scaling along $\Gamma(\theta)$, and (c) provides a schematic summary of the coordinated re-weighting of $\{Bo, Pe, Da\}$ with inclination.

The shape of this trajectory is generic at leading order within the present lubrication framework, in the sense that it follows directly from the structure of the lubrication flux, whereas the position of any specific physical system along it depends on material parameters such as viscosity, intermolecular constants, diffusivity and reaction rates.

Thus, rather than claiming that all thin-film systems evolve identically, we emphasize that inclination constrains the leading-order coupling of Bo, Pe and Da, while material properties determine the quantitative location along the trajectory. This leading-order coupling arises directly

 doi:10.20944/preprints202603.2106.v1

from the structure of the lubrication flux: gravitational forcing grows with inclination (Bo ↑), advection strengthens accordingly (Pe ↑), and the advective enhancement weakens the relative importance of reaction (Da ↓). Together, these coordinated shifts reorganize the balance between drainage, transport and confined reactivity.

The resulting leading-order inclination-driven trajectory provides a compact and physically transparent representation of the underlying dynamics. It captures the progressive transition from capillarity-dominated flow at low inclination to advection-dominated drainage at high inclination and simultaneously explains the loss of reactive confinement and the shortening of residence times observed in Section 5. The trajectory therefore offers a unifying perspective on inclined thin-film behavior, linking geometry, force balance and transport hierarchy within a single mathematical structure.

A key consequence is that inclination does not explore the full (Bo, Pe, Da) space. Instead, it constrains the dynamics to a one-dimensional trajectory $\Gamma(\theta)$, along which regime transitions occur in a fixed order. This reduction of apparent complexity is a central organizing consequence of the present framework

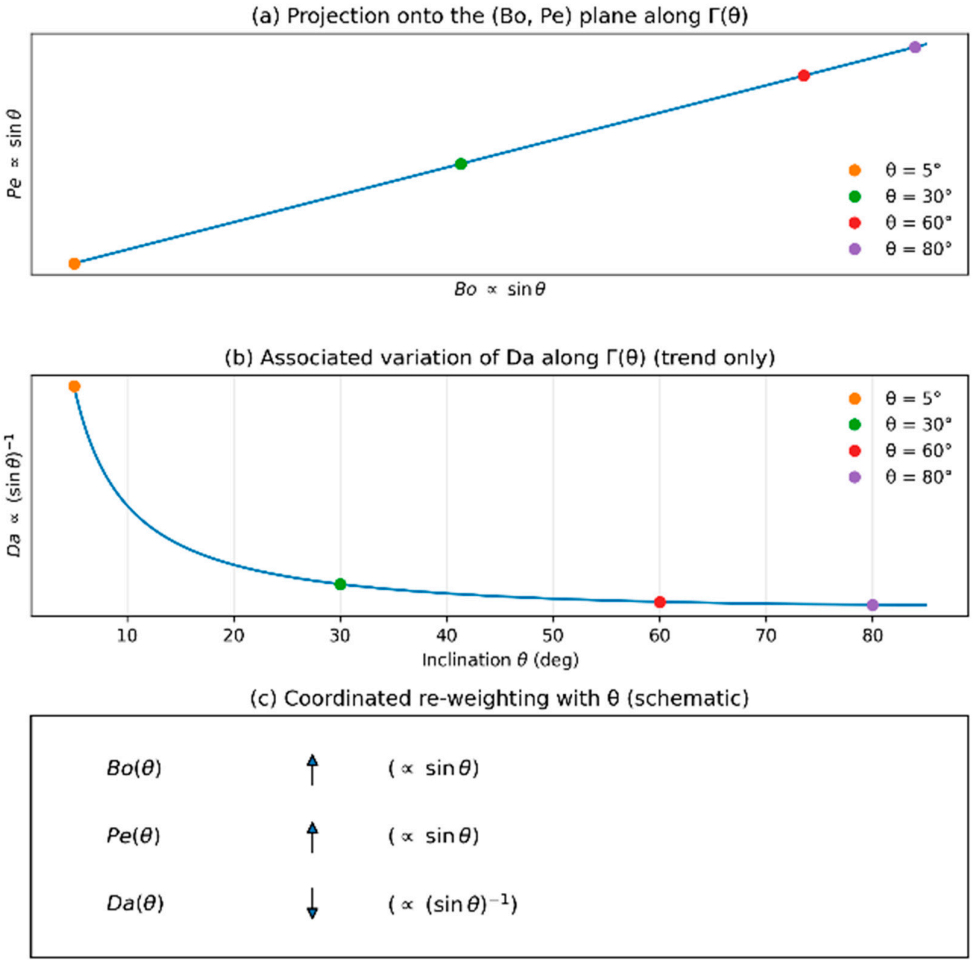

Figure 2. Geometry-imposed inclination-driven trajectory in the $\{Bo, Pe, Da\}$ space. (a) Projection onto the (Bo, Pe) plane along $\Gamma(\theta)$. (b) Associated $Da(\theta)$ scaling along the same path. (c) Schematic summary of the coordinated re-weighting with θ, highlighting that inclination constrains the dynamics to a one-parameter manifold rather than exploring the full parameter space.

3.6. Representative Parameterization and Crossover Angles

 doi:10.20944/preprints202603.2106.v1

To provide a representative quantitative anchor for the leading-order framework, we consider an ultrathin atmospheric electrolyte film at 25 °C. The fluid properties are taken as representative aqueous values, namely $\rho = 997\,\mathrm{kg\,m^{-3}}$, $\mu = 0.89 \times 10^{-3}\,\mathrm{Pa\,s}$, and $\gamma = 71.97 \times 10^{-3}\,\mathrm{N\,m^{-1}}$, consistent with standard thermophysical data for water [21], while the molecular diffusivity is taken as $D = 2.03 \times 10^{-9}\,\mathrm{m^2\,s^{-1}}$, a representative value commonly adopted for chloride transport in aqueous media [22]. The characteristic thickness $H = 1\,\mu\mathrm{m}$ is adopted as a representative thin-film scale relevant to atmospheric corrosion [11,12], while $L = 1\,\mathrm{mm}$ is introduced here as a representative surface-transport length for the illustrative calculation. The complete parameter set is summarized in Table 1.

For this representative parameter set, the reference drainage velocity scale is

$$U_0 = \frac{\rho g H^2}{3\mu} \approx 3.66 \times 10^{-6}\,\mathrm{m\,s^{-1}},$$

which gives

$$Pe_0 = \frac{U_0 L}{D} \approx 1.80, Bo_0 = \frac{\rho g H^2}{\gamma} \approx 1.36 \times 10^{-7}.$$

Accordingly, the inclination-dependent drainage velocity becomes

$$U_\theta = U_0 sin\,\theta,$$

so that

$$Pe(\theta) \approx 1.80\,sin\,\theta.$$

The transport crossover defined by $Pe = 1$ therefore occurs at

$$\theta_{Pe} \approx 33.7°.$$

To illustrate the reactive branch of the trajectory, we further adopt here a representative first-order reaction rate $k = 10^{-3}\,\mathrm{s^{-1}}$, used only for the illustrative crossover estimate. This yields

$$Da(\theta) \approx \frac{0.273}{\sin\theta}.$$

The corresponding reactive crossover $Da = 1$ then occurs at

$$\theta_{Da} \approx 15.8°.$$

The resulting inclination-dependent evolution of $Pe(\theta)$ and $Da(\theta)$ is shown in Figure 3. The intersections with the unity threshold make the crossover angles θ_{Da} and θ_{Pe} explicit and show that, for this representative case, the reactive crossover precedes the transport crossover. In other words, the system first exits the reaction-dominated regime and only at larger inclinations enters the mixed advection–diffusion regime. At the same time, the Bond number remains very small throughout, since $Bo_0 \approx 1.36 \times 10^{-7}$, indicating that the film remains strongly capillary-dominated even though transport and reactive accessibility are substantially reorganized by inclination.

This example is not intended as a system-specific calibration, but rather as a representative quantitative illustration of the crossover structure implied by the inclination-driven trajectory $\Gamma(\theta)$.

Table 1. Representative parameters used to illustrate the inclination-driven crossover structure.

Parameter	Value
H	1 μm
L	1 mm
ϱ	997 kg m^{-3}
μ	0.89×10^{-3} Pa s
γ	71.97×10^{-3} N m^{-1}
D	2.03×10^{-9} m^2 s^{-1}
k [a]	10^{-3} s^{-1}

[a] Adopted here only to illustrate of the reactive branch.

 doi:10.20944/preprints202603.2106.v1

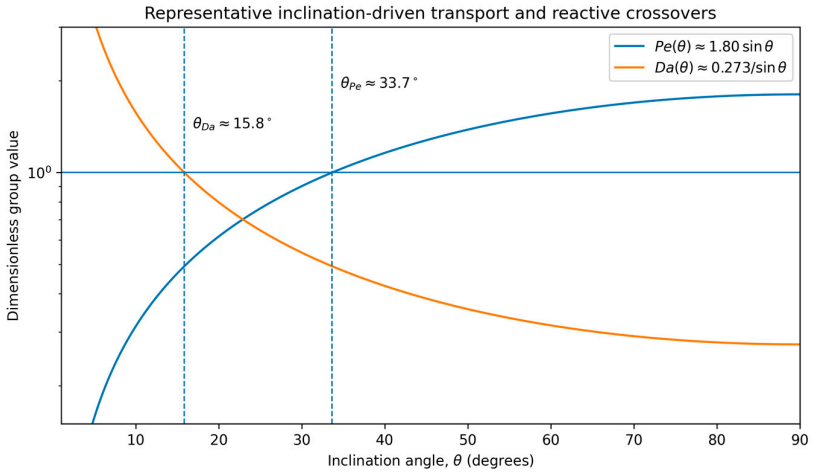

Figure 3. Representative inclination-driven transport and reactive crossovers for the parameter set listed in Table 1. The curves show $Pe(\theta) \approx 1.80\sin\theta$ and $Da(\theta) \approx 0.273/\sin\theta$. The horizontal line at unity identifies the crossover angles $\theta_{Da} \approx 15.8^\circ$ and $\theta_{Pe} \approx 33.7^\circ$, corresponding to the onset of transport-limited behavior and mixed advection–diffusion transport, respectively.

3.7. Implications for Film Stability, Transport and Rupture

The inclination-driven variations of Bo, Pe and Da summarized by the leading-order trajectory $\Gamma(\theta)$ have direct consequences for film stability, drainage dynamics and confined transport. As θ increases, gravitational forcing strengthens through Bo, advection becomes progressively dominant through Pe, and the relative importance of reaction diminishes through Da. These coordinated shifts reorganize the hierarchy of physical processes that govern thin-film behaviour.

For stability, an increase in Bo accelerates thinning and promotes earlier access to regimes in which intermolecular attractions dominate. This leads to reduced rupture times and asymmetric dewetting fronts, consistent with the gravitational bias introduced in Section 2 and with theoretical predictions for gravity-driven front propagation and instability asymmetry [4,8].

For transport, the increase in Pe shortens residence times and enhances the longitudinal advection of solute, weakening the ability of diffusion to maintain uniform concentration profiles. Confined electrostatics and near-surface interactions become less effective as the film is rapidly displaced downslope.

For reactions, the decrease in Da shifts the system from reaction-dominated behavior at low inclination toward a transport-limited regime at higher inclination. This transition reduces the duration over which solutes can interact within confined, high-resistivity regions and therefore suppresses sustained reactive pathways.

Together, these trends suggest an inclination-controlled classification of thin-film regimes, expressed through measurable crossover conditions in (Bo, Pe, Da) space. This deterministic structure provides the foundation for the stochastic wetting analysis developed in Section 4, where inclination-driven variations in drainage rate and residence time control the statistics of wet–dry cycling and the long-time persistence of reactive intervals.

4. Stochastic Wetting and Time-of-Wetness Dynamics

Thin films exposed to atmospheric forcing rarely evolve as continuous layers. Instead, they undergo intermittent cycles of formation, drainage, rupture and re-wetting driven by humidity fluctuations, aerosol deposition and environmental noise. While the deterministic equations of Section 2 describe the deterministic dynamics of the film thickness, they cannot capture the discrete transitions between wet and dry states that dominate long-time surface behavior. A stochastic

 doi:10.20944/preprints202603.2106.v1

description is therefore required to represent the intermittent nature of atmospheric wetting, particularly on inclined substrates where drainage is strongly enhanced.

Inclination modifies these transitions by reorganizing the drainage flux, accelerating access to rupture thresholds and reducing the residence time of liquid films. The combined deterministic–stochastic structure provides a physically grounded framework for understanding the observed decrease in time-of-wetness with increasing inclination.

4.1. Deterministic Thin-Film Dynamics and Rupture Thresholds

The deterministic dynamics of the film thickness are governed by the lubrication-based thin-film equation

$$\partial_t h + \partial_x q = S(x,t), \quad (19)$$

which describes the continuous thinning of the film between wetting events. Rupture occurs when the local thickness reaches the critical value h_{crit}, set by the balance between van der Waals attraction and capillary curvature. This threshold marks the limit of metastability for ultrathin films and determines the termination of a wet interval in the absence of re-wetting.

As shown in Sections 2 and 3, the gravitational contribution to the flux grows with inclination through the gravitational forcing $\rho g \sin\theta$ in the lubrication flux (Section 2), and equivalently through the inclination dependence of the relevant dimensionless groups introduced in Section 3. The increased downslope advection accelerates thinning and causes the deterministic trajectory $h(t)$ to reach h_{crit} more rapidly as θ increases. In particular, in the drainage-dominated limit the characteristic film-loss time scales as $t_{drain}(\theta) \sim L/U_\theta$, with $U_\theta \propto \sin\theta$, implying a monotonic decrease of $t_{drain}$with inclination. Inclination therefore shortens the deterministic component of the wet-state lifetime, independently of environmental factors such as humidity or aerosol deposition.

The inclination dependence of the drainage time plays a central role in the stochastic framework developed in Section 4.2: it sets the scale for the drying rate λ_{dry}, which increases monotonically with θ. The deterministic thinning dynamics therefore provide the physical basis upon which the stochastic wet/dry transitions are built.

4.2. Stochastic Transition Between Wet and Dry States

Environmental forcing introduces intrinsic randomness into film re-formation events, primarily through humidity fluctuations, aerosol deposition and vapor-phase transport.

To capture this behavior, the surface is idealized as a two-state stochastic process in which the interface alternates between

- a wet state (W), where a continuous or metastable film exists, and
- a dry state (D), where the film has ruptured or is absent.

Transitions between these states occur with rates

$$W \xrightarrow{\lambda_{\mathrm{dry}}} D, D \xrightarrow{\lambda_{\mathrm{wet}}} W,$$

where λ_{dry} is the drying or rupture rate, and λ_{wet} is the re-wetting rate associated with condensation or deliquescence [19,20].

Inclination modifies these rates asymmetrically. As shown in Sections 2 and 3, the gravitational contribution to the flux increases monotonically with $\mathrm{Bo}\sin\theta$, reducing the deterministic drainage time of Section 4.1 and thereby increasing λ_{dry}. In contrast, λ_{wet} depends primarily on humidity, temperature and vapor transport, and is only weakly sensitive to θ [11]. This asymmetry—an inclination-enhanced drying rate together with an approximately inclination-independent wetting rate—is the stochastic counterpart of the inclination-driven re-weighting of the Bond, Péclet and Damköhler numbers established in Section 3.

The competition between λ_{dry} and λ_{wet} governs the statistics of intermittent wetting. In particular, the steady-state wet-state probability is

$$P_{\mathrm{wet}} = \frac{\lambda_{\mathrm{wet}}}{\lambda_{\mathrm{wet}}+\lambda_{\mathrm{dry}}}, \quad (20)$$

 doi:10.20944/preprints202603.2106.v1

which decreases systematically with inclination because $\lambda_{\mathrm{dry}}(\theta)$ grows while λ_{wet} remains nearly constant. This two-state Markov process also yields closed-form dwell-time statistics: the mean wet-interval duration is $\langle t_W \rangle = 1/\lambda_{dry}$, and the mean dry-interval duration is $\langle t_D \rangle = 1/\lambda_{wet}$. Inclination therefore reduces $\langle t_W \rangle$ deterministically through $\lambda_{dry}(\theta)$, while leaving $\langle t_D \rangle$ primarily controlled by environmental forcing.

This provides a physically grounded explanation for the pronounced reduction in wet-state persistence observed experimentally in inclined electrolyte films [12], without invoking any chemistry-specific mechanisms.

The structure of this two-state stochastic pathway, together with the deterministic–stochastic closure $\lambda_{dry}(\theta) \sim t_{drain}(\theta)^{-1}$, is summarized in Figure 4.

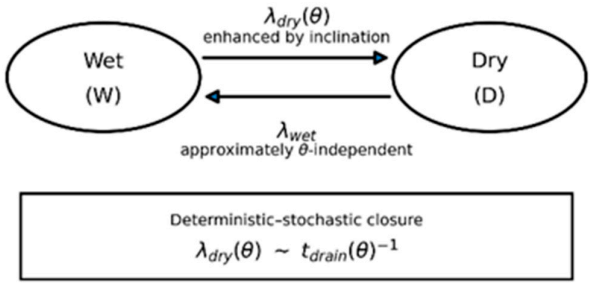

Figure 4. Two-state Markov model for wet–dry intermittency. W denotes the wet (film-present) state and D the dry/ruptured (film-absent) state**.** The drying/rupture transition $W \to D$ occurs at rate $\lambda_{dry}(\theta)$, enhanced by inclination, while re-wetting $D \to W$ occurs at rate λ_{wet}, taken approximately independent of θ. The deterministic–stochastic closure is $\lambda_{dry}(\theta) \sim t_{drain}(\theta)^{-1}$.

The Stochastic formulation thus complements the deterministic dynamics by providing a quantitative description of how inclination reshapes the balance between rupture and re-formation events, establishing the foundation for the time-of-wetness analysis in Section 4.3.

This two-state model is intentionally minimal and assumes Poissonian (memoryless) transitions, with constant wetting and drying rates. In this formulation, the $W \leftrightarrow D$ dynamics constitute a Markov process with exponential waiting times, providing a mean-field description that neglects temporal correlations and long-tailed statistics. Such a closure is appropriate for capturing inclination-controlled shifts in the average wet persistence, but it does not resolve potential non-Markovian effects, such as heavy-tailed waiting times or humidity-driven correlations associated with environmental fluctuations or substrate heterogeneity. These extensions lie beyond the scope of the present work.

4.3. Wet-State Persistence and Time-Of-Wetness

The stochastic description introduced in Section 4.2 determines the persistence of wet states through the competition between the drying and re-wetting pathways. In the long-time limit, the wet-state probability is fully controlled by the ratio $\lambda_{\mathrm{wet}}/\lambda_{\mathrm{dry}}$. Since inclination affects only the drying pathway—by shortening the deterministic drainage time of Section 4.1—the wet-state probability inherits a strict geometric dependence, decreasing monotonically with θ.

An illustrative prediction of this monotonic dependence is shown in Figure 5.

 doi:10.20944/preprints202603.2106.v1

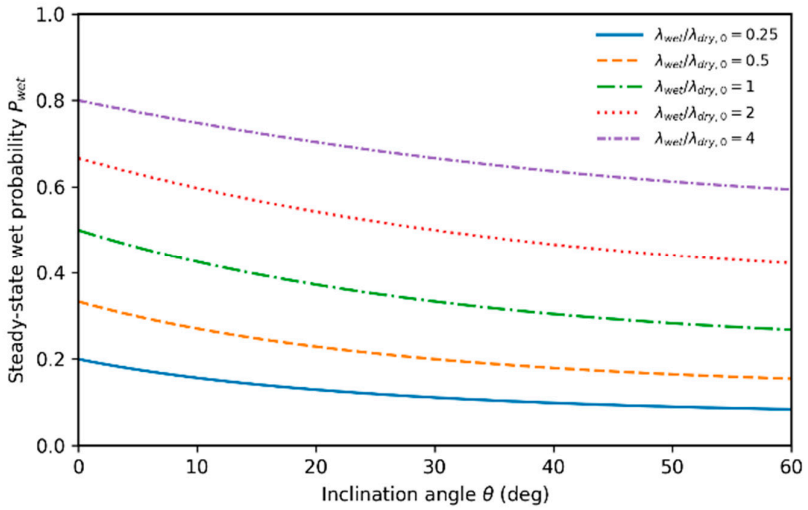

Figure 5. Steady-state wet-state probability $P_{wet} = \lambda_{wet}/(\lambda_{wet} + \lambda_{dry}(\theta))$ as a function of inclination angle θ for several ratios $\lambda_{wet}/\lambda_{dry,0}$ (legend), where $\lambda_{dry,0} \equiv \lambda_{dry}(\theta = 0)$. Inclination enhances the drying pathway by increasing $\lambda_{dry}(\theta)$ (through the shorter deterministic drainage time), while λ_{wet} is taken approximately independent of θ, producing a monotonic decline in wet-state persistence. The qualitative trend is robust to the specific functional form of $\lambda_{dry}(\theta)$, provided λ_{dry} increases monotonically with inclination.

The time-of-wetness (TOW), defined as the fraction of a long interval during which the surface remains wet, coincides with this steady-state wet probability for any stationary two-rate process. Thus, TOW decreases systematically with inclination, reflecting the geometry-driven amplification of the drying pathway rather than any chemistry-specific mechanism. A characteristic crossover inclination $\theta*$ may be defined by the condition $\lambda_{dry}(\theta*) \approx \lambda_{wet}$, marking the transition from predominantly wet to predominantly dry surface occupancy under otherwise unchanged environmental forcing. This behavior is consistent with the pronounced decline in wet-state persistence observed experimentally for electrolyte films on inclined metallic substrates [11,12].

This probabilistic viewpoint completes the connection between deterministic drainage, stochastic rupture and macroscopic wet/dry statistics, providing the basis for the stability and transport consequences examined in Section 5.

4.4. Coupling Deterministic Dynamics to Stochastic Transitions

The stochastic transitions characterized by the rates λ_{dry} and λ_{wet} acquire physical meaning only when linked to the deterministic thinning behavior established in Section 4.1. The drainage time $t_{\mathrm{drain}}(\theta)$, defined as the time for a continuous film to reach its rupture threshold, sets the natural scale for transitions out of the wet state. Consequently,

$$\lambda_{\mathrm{dry}} \sim t_{\mathrm{drain}}^{-1}, \quad (21)$$

so that inclination modifies the drying pathway entirely through its influence on the deterministic fluxes derived in Section 2 and the dimensionless re-weighting discussed in Section 3. This deterministic closure is central: it fixes the entire inclination dependence of the stochastic model through $t_{drain}(\theta)$, rather than treating $\lambda_{dry}(\theta)$ as an empirical fitting function.

In contrast, the re-wetting rate is set by vapor-phase processes, condensation kinetics and ambient humidity fluctuations [19,20], none of which couple directly to gravitational asymmetry. The stochastic model therefore inherits a unidirectional sensitivity: inclination accelerates drying but leaves re-wetting largely unchanged.

This separation of roles is essential. It provides a mechanistic interpretation for why wet/dry cycling becomes increasingly intermittent with increasing θ, and why time-of-wetness decreases despite unchanged environmental forcing. The deterministic–stochastic link also ensures that

 doi:10.20944/preprints202603.2106.v1

statistical quantities such as the wet-state probability, wet-interval distribution, and the long-time TOW (Section 4.3) are governed by geometric rather than material parameters.

4.5. Implications for Interfacial Reactivity and Transport

The intermittent wetting generated by the dynamics of Sections 4.1–4.4 has direct consequences for transport and reactive processes within ultrathin films. Because solute retention, electrostatic confinement and reaction kinetics all depend on the duration and continuity of the wet state, the progressive decline in wet-state persistence with inclination produces a systematic reorganization of interfacial behavior.

In the low-inclination regime, long wet intervals and relatively infrequent drying events allow ionic confinement and concentration gradients to develop, favoring reaction pathways that require sustained film continuity. As inclination increases, the shortening of wet intervals limits solute residence time and weakens electrostatic confinement, shifting the interfacial response toward transport-controlled, short-residence-time regimes. These effects arise directly from the inclination-controlled imbalance between λ_{dry} and λ_{wet}, rather than from any material-specific chemistry. This interpretation aligns with experimental observations of reduced wet-state longevity and intermittent reactivity on inclined metallic substrates [11,12].

Stochastic intermittency therefore represents the final element in the multiscale picture developed in this section: deterministic thinning sets rupture timing, stochastic forcing governs re-wetting, and inclination biases the entire process toward rapid cycling. Together, these effects provide a leading-order basis for inclination-dependent intermittency metrics, through $\lambda_{dry}(\theta)$ and $P_{wet}(\theta)$, which directly constrain the stability, drainage and transport consequences analyzed in Section 5. In this sense, the representative crossover structure introduced in Section 3.6 complements the stochastic description by showing that the transport and reactive transitions induced by inclination can occur within experimentally relevant angular ranges.

More detailed stochastic structure, such as long-tailed wetting intervals, state-dependent rates, or humidity-correlated transitions, falls outside the scope of the present mean-field description and constitutes a natural extension for future work.

5. Physical Consequences of the Inclination-Driven Trajectory $\boldsymbol{\Gamma(\theta)}$

The dimensionless structure derived in Section 3 and the deterministic–stochastic coupling introduced in Section 4 together define a unified picture of how inclination reorganizes thin-film behavior. In particular, the inclination-driven trajectory $\Gamma(\theta)$ provides a compact organizing framework for interpreting how the governing balances evolve with geometry. Rather than acting as a secondary perturbation, inclination systematically reorders the competition among capillarity, intermolecular forces, drainage, transport, and wet-state persistence. This section extracts the main physical consequences of that trajectory, focusing on five interconnected aspects: stability, drainage and thinning, transport regimes, reactive confinement, and long-time intermittency.

5.1. Stability Regimes Under Inclination

The stability of a thin film on an inclined substrate results from the competition between capillary curvature, intermolecular interactions and the gravitational asymmetry introduced by θ. Linearising the hydrodynamic flux of Section 2 about a uniform base state of thickness H yields the dispersion relation

$$\sigma(k) = -k^4 + \Pi'(H)\, k^2 + i(\mathrm{Bo}\sin\theta)\, k, \quad (22)$$

where $\sigma(k)$ is the (generally complex) temporal growth rate of a Fourier mode of wavenumber k, and $\Pi'(H)$ denotes the derivative of the disjoining pressure evaluated at the base thickness. Capillarity contributes to the stabilizing term $-k^4$, intermolecular forces contribute the destabilizing term proportional to k^2, and inclination introduces a linear drift term $\propto i\,k$ that biases the disturbance toward downhill-propagating (travelling) modes rather than changing the amplification

 doi:10.20944/preprints202603.2106.v1

mechanism itself. The combined effect reshapes both the route to rupture and the spatial structure of the most unstable modes.

For horizontal substrates ($\theta = 0$), the spectrum is symmetric in k, and stability is determined solely by the balance between capillarity and intermolecular interactions, recovering the classical result for thin-film rupture [7,9]. This baseline behavior corresponds to the standard long-wave instability structure examined in lubrication-type analyses [8]. Inclination breaks this symmetry: the additional term $(\mathrm{Bo}\sin\theta)k$ introduces a downhill drift of unstable modes and converts symmetric dewetting patterns into travelling disturbances, while the onset of long-wave amplification remains controlled by the capillarity–disjoining balance. As a result, perturbations with positive k (downslope) exhibit downslope propagation, while upslope modes are effectively suppressed by the convective bias. This spectral asymmetry provides a mechanistic explanation for the directionality observed in experiments on inclined wetting films [12] and coating flows [4,5].

The inclination dependence of the maximum growth rate follows directly from the dispersion relation. For the growth-controlling real part, $\sigma_r(k) = -k^4 + \Pi'(H)k^2$, the most amplified mode satisfies $k_{max} = \sqrt{\Pi'(H)/2}$ and $\sigma_{max} = \Pi'(H)^2/4$, whereas inclination controls the corresponding drift speed through the $i(Bo\sin\theta)k$ term. Thus, in this leading-order formulation, inclination primarily changes the convective character of the instability (propagation bias) rather than the growth-rate envelope $\sigma_r(k)$. Accordingly, changes in apparent peak position or cutoff with θ should be interpreted as schematic/illustrative unless additional θ-dependent physics enters σ_r (e.g., through a θ-dependent base state H or additional transport couplings). This separation between amplification (σ_r) and drift (σ_i) is summarized schematically in Figure 6.

This inclination-induced restructuring of the instability landscape establishes the foundation for the drainage, transport and reactive consequences developed in Sections 5.2–5.5.

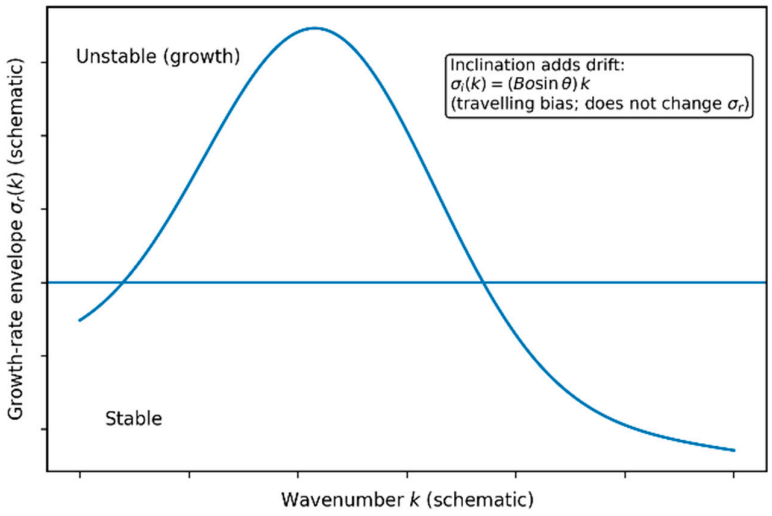

Figure 6. Schematic growth-rate envelope $\sigma_r(k)$ for a uniform base film, showing the long-wave amplification band ($\sigma_r > 0$) and the most amplified mode (peak) set by capillarity and disjoining pressure. Inclination does not modify $\sigma_r$in Eq. (22) but adds a drift term $\sigma_i(k) = (Bo\sin\theta)k$ that breaks the $\theta = 0$ symmetry and biases disturbances toward downhill propagation.

5.2. Drainage and Thinning Under Inclination

Inclination alters the drainage behavior of thin films in a systematic and theoretically transparent manner. Because the gravitationally induced flux term $\mathrm{Bo}\sin\theta$ enters the hydrodynamic equation linearly, its influence propagates directly into the thinning kinetics of the film. This linear dependence is the same one that governs the inclination-driven coupling of the Bond, Péclet and Damköhler numbers in Section 3.5, so the drainage pathway reflects the underlying structure of the nondimensional trajectory.

 doi:10.20944/preprints202603.2106.v1

For a finite film segment draining toward an edge (or a representative control volume with net outflow), the leading-order drainage law obtained from the lubrication equation reduces to

$\partial_t h \approx -C\, h^3\, \mathrm{Bo}\, \sin\theta$, (23)

where C collects viscosity and geometric constants.

This expression encapsulates three key consequences:

1. Accelerated thinning with inclination:

Since the gravitational contribution scales as $\sin\theta$, the drainage time obeys

$t_{\mathrm{drain}}(\theta) \propto (\sin\theta)^{-1}$ (24)

(for fixed H, L, μ). Thus, even moderate inclination substantially shortens the film lifetime, a tendency consistent with the deterministic pathways leading to rupture discussed in Section 5.1.

This inclination dependence is the drainage counterpart of the coordinated scaling $Pe \propto \sin\theta$ appearing in the nondimensional formulation.

2. Enhanced sensitivity in the ultrathin regime:

As the film approaches nanometric thicknesses, the cubic dependence on h makes the dynamics increasingly stiff, so that even small reductions in thickness produce disproportionately large increases in the thinning rate. Consequently, inclination-induced acceleration is magnified near the disjoining-pressure–dominated regime, making rupture markedly more abrupt than in horizontal geometries [2].

3. Earlier loss of continuity and reduced recovery intervals:

Because evaporation competes with downhill drainage, the accelerated thinning induced by inclination shifts the balance strongly toward rupture.

Even before stochastic re-wetting is considered (Section 4), the deterministic trajectory reaches the rupture threshold h_{crit} more rapidly.

The subsequent re-formed films originate from progressively thinner initial states, reinforcing the cycle of short-lived wet intervals.

Together, these drainage characteristics supply the deterministic backbone that feeds into the stochastic transitions of Section 4.

The inclination-controlled reduction of t_{drain} is therefore not a system-specific effect, but the leading-order drainage counterpart of the coordinated trajectory in the $\{Bo, Pe, Da\}$ space derived in Section 3.

5.3. Transport Regimes: Advection, Diffusion, and Confinement

The dimensionless analysis of Section 3 showed that inclination increases the Péclet number through the scaling $Pe \propto \sin\theta$.

This single geometric modification reshapes the balance between advection and diffusion within the film across three distinct regimes.

These regimes arise from the competition between downhill advection $\mathrm{u} = \mathrm{q/h}$ and transverse diffusion and are further modulated by the thickness-dependent confinement of ionic mobility [2,14].

The resulting geometry-induced transport regimes, and the associated crossover sequence along $Pe(\theta)$, are summarized schematically in Figure 7.

 doi:10.20944/preprints202603.2106.v1

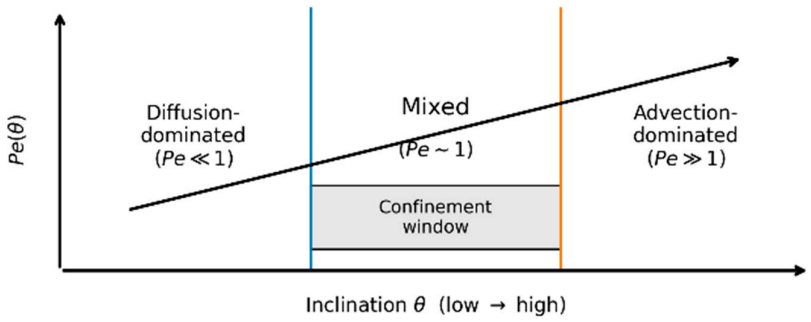

Figure 7. Schematic transport-regime sequence along inclination θ, reflecting the geometry-imposed increase of $Pe(\theta)$. As θ increases, the system crosses from diffusion-dominated ($Pe \ll 1$) to mixed ($Pe \sim 1$) and advection-dominated ($Pe \gg 1$) transport. The shaded interval (confinement window) marks the range of inclinations over which ionic mobility remains strongly confined, indicating that strong confinement and transport asymmetry can coexist over a limited parameter window.

At low inclination, transport is diffusion-dominated, since the advective flux remains weak and $Pe \ll 1$. Under these conditions, spatial concentration gradients relax faster than they are generated, so solutes remain confined within the film and their residence time is governed primarily by the local thickness and molecular diffusivity. Electrostatic confinement is strong in this regime, because double-layer overlap suppresses mobility and favors transport-limited reactions. As θ increases, the advective velocity grows proportionally to $sin\,\theta$, eventually bringing the system to $Pe \sim \mathcal{O}(1)$, where a mixed advection–diffusion regime emerges. Diffusion can no longer fully eliminate the concentration gradients induced by downhill drainage, and longitudinal compositional variations, solute accumulation zones, and reaction rates coupled to the hydrodynamic timescale begin to develop. This marks the onset of geometry-induced transport asymmetry, whereby even an otherwise nearly uniform film may preferentially carry solutes toward the downhill edge. At larger inclinations, $Pe \gg 1$ and advection becomes dominant: solutes are swept downslope faster than they can redistribute, leading to a sharp reduction in residence time. At the same time, electrostatic confinement weakens because rapid thinning (Section 5.2) drives the film below the stable-confinement regime before diffusive equilibration can occur. In this limit, the reaction dynamics are governed less by local kinetics than by the rate at which material can be supplied to, or retained within, the thinning film. The confinement window highlighted in Figure 7 therefore identifies the range of inclinations over which confinement can still persist despite the progressive increase in transport asymmetry.

5.4. Inclination Effects on Reactive Confinement

Although the formulation is general, electrolyte films offer a particularly clear illustration of how inclination reorganizes reactive behavior.

Because the Damköhler number satisfies

$$\mathrm{Da}(\theta) \propto (\sin\,\theta)^{-1}, \quad (25)$$

increasing inclination reduces the time available for ions to remain confined within the liquid layer. This effect is reinforced by two mechanisms previously established in Sections 4 and 5.2: (i) the shortening of wet intervals caused by inclination-enhanced drainage, and (ii) the weakening of electrostatic confinement as the film is driven rapidly into the ultrathin regime.

The combined consequence is a transition from long-residence-time, confinement-dominated behavior at low inclination to short-residence-time, intermittency-limited behavior at high inclination. Reaction pathways requiring sustained connectivity—such as those involving concentrated boundary layers or strongly overlapped double layers—are progressively suppressed.

 doi:10.20944/preprints202603.2106.v1

Instead, reactivity becomes governed by the supply of material to the thinning film and by the stochastic occurrence of short wet intervals. These effects do not rely on electrolyte-specific chemistry: they arise generically from the re-weighting of Da, Pe and the rupture rate with θ.

This inclination-driven shift in confinement and reactivity provides a physical interpretation for the reduced wet-state persistence and intermittent electrochemical activity reported experimentally on inclined metallic surfaces [11,12].

5.5. Long-Time Intermittency and Wet-State Persistence

The combined deterministic and stochastic descriptions developed in Sections 2–4 reveal a coherent and geometry-driven reorganization of thin-film behavior under inclination. As the Bond and Péclet numbers increase with θ, deterministic thinning accelerates, rupture occurs earlier, and the drying pathway strengthens relative to the re-wetting pathway. The stochastic model of Section 4 shows that this imbalance raises the drying rate $\lambda_{\mathrm{dry}}(\theta)$ while leaving λ_{wet} essentially controlled by humidity and vapour transport. The consequence is a systematic decline of the wet-state probability and a transition to highly intermittent wet/dry dynamics.

In this intermittent regime, the long-time behavior of the film is governed by sporadic and short-lived wet intervals separated by extended dry periods. The hydrodynamic structure of the film becomes increasingly asymmetric: downhill thinning accelerates with *Pe*, confinement breaks down earlier, and the residual film thickness approaches the rupture threshold more rapidly. Transport processes reflect the same geometric influence. At modest inclination, mixed advection–diffusion behavior persists, but at large θ the dynamics become decisively advection-dominated, with solutes swept downslope before diffusive redistribution can occur.

These inclination-induced changes have broad implications for reactive and confined films. Intermittency truncates residence times; interrupts extended reactive phases and suppresses steady confined-electrostatic regimes. The interface becomes reactive only during brief wet windows, and the corresponding reaction pathways become strongly history-dependent.

This global behavior accelerated thinning, diminished wet-state persistence, loss of confinement, and the emergence of strong intermittency—is a generic consequence of the inclination-driven hierarchy of dimensionless groups, not of any particular chemistry.

These coupled trends predict measurable signatures: a monotonic decrease of $P_{wet}(\theta)$, a reduction of mean wet-interval duration $\langle t_W \rangle = 1/\lambda_{dry}(\theta)$, and a transition from $Pe \ll 1$ to $Pe \gg 1$ transport as θ increases.

6. Discussion

The framework developed in this work unifies the hydrodynamic, interfacial, gravitational and stochastic mechanisms governing thin films on inclined substrates. By deriving the governing equations from first principles and analyzing their dimensionless structure, we have shown that inclination acts not merely as a geometric parameter but as a symmetry-breaking field that modifies drainage, stability and transport in a coordinated manner. This reorganization is encoded in a single inclination-driven trajectory in the (Bo, Pe, Da) parameter space, which emerges directly from the structure of the lubrication-type equations and is therefore only weakly dependent, at leading order, on system-specific material properties in its functional form, although the location along the trajectory remains material-dependent.

This geometric control manifests across all levels of dynamics. Deterministically, increased inclination enhances gravitational forcing, accelerates thinning, shifts instability thresholds and shortens the residence time of solutes in confined ultrathin regions. Stochastically, the strengthened drainage pathway increases the drying rate while leaving the re-wetting pathway largely unaffected, thereby reducing the steady wet-state probability and enhancing the intermittency of wet/dry cycling. Together, these deterministic and stochastic consequences generate the characteristic features of inclined films: rapid thinning events, asymmetric profiles, premature loss of confinement and temporally fragmented reactive phases.

 doi:10.20944/preprints202603.2106.v1

The representative parameterization introduced in Section 3.6 makes this ordering quantitatively explicit. For the illustrative ultrathin electrolyte film considered there, the reactive crossover $\theta_{Da} \approx 15.8^{\circ}$ precedes the transport crossover $\theta_{Pe} \approx 33.7^{\circ}$, while the corresponding Bond number remains far below unity. This representative example shows that substantial transport and reactive reorganization can occur even within a strongly capillary-dominated regime, and it provides a concrete quantitative anchor for the leading-order crossover structure summarized by $\Gamma(\theta)$.

Representative experimental systems reported in [11,12] appear to fall within the same region of the inclination-driven trajectory in $\{Bo, Pe, Da\}$ space, which is consistent with the leading-order scaling proposed here.

Although the formulation is general, its qualitative implications are consistent with the physical conditions reported for atmospheric electrolyte films. Representative orders of magnitude, typical film thicknesses of $H \approx 10$–100 nm, lateral length scales of $L \approx 1$–10 mm, and gravitationally driven drainage velocities in the range 10^{-6}–$10^{-4}\ \mathrm{m\,s^{-1}}$, all compatible with the regimes discussed in [11,12], place such systems in the low-Bond-number range ($Bo \approx 10^{-6}$–10^{-4}), with moderate-to-high Péclet numbers ($Pe \approx 1$–100) and order-unity to moderately varying Damköhler numbers. These values are broadly aligned with the inclination-dependent trends identified in Section 3, as well as with the representative crossover structure illustrated in Figure 3, supporting the physical relevance of the framework while remaining within its intended role as a leading-order, conceptual description rather than a detailed quantitative prediction.

The stochastic component of the model is deliberately minimal: the wet-to-dry and dry-to-wet transitions are treated as a two-state Poisson process with constant rates. This Markov assumption provides a transparent mean-field description of intermittent wetting, but it does not attempt to capture heavy-tailed waiting-time distributions or humidity-driven temporal correlations. Such effects, often observed in environmental systems, could be incorporated in future work through renewal processes or continuous-time random-walk formulations.

The unified structure presented here also identifies several directions for further development. Extending the analysis to two- and three-dimensional geometries would enable the study of transverse instabilities, rivulet formation and interactions between gravitational forcing and contact-line pinning. Introducing substrate heterogeneity or patterned wettability could reveal non-trivial couplings between microscopic pinning and macroscopic symmetry breaking. Coupling the present framework to detailed electrochemical kinetic models would clarify how intermittent wetting shapes reactive pathways, especially under cyclic humidity forcing. Finally, integrating realistic stochastic humidity profiles may reproduce long-tailed wet-interval distributions observed in environmental systems.

The present work provides a coherent physical description of thin films under geometric asymmetry, bridging hydrodynamics, intermolecular forces, confined transport and stochastic wetting within a single mathematical structure. The inclination-driven trajectory offers a compact conceptual lens through which to interpret a broad spectrum of interfacial phenomena across soft matter, thin-film hydrodynamics, coating flows, microfluidics and environmentally driven surface processes.

7. Conclusions

We have developed a unified theoretical framework that couples hydrodynamics, intermolecular forces, gravitational asymmetry and stochastic wetting to describe the behavior of thin films on inclined substrates. The formulation, derived from first principles, identifies the key dimensionless groups governing the system and shows how inclination systematically reweights the balance between capillarity, van der Waals forces, drainage and transport.

Inclination enhances the drying pathway without significantly affecting re-wetting, leading to a monotonic reduction of wet-state persistence and the emergence of strongly intermittent wet/dry dynamics. These effects arise directly from the structure of the lubrication-type equations and the

 doi:10.20944/preprints202603.2106.v1

associated scalings of the Bond, Péclet and Damköhler numbers, rather than from chemistry-specific assumptions.

A representative quantitative parameterization further shows that this inclination-driven structure yields explicit crossover angles for reactive-confinement loss and transport reorganization, thereby complementing the general scaling analysis with a concrete regime illustration. In the representative case examined here, the system remains strongly capillary-dominated while still undergoing ordered Da- and Pe-controlled transitions as the inclination increases.

Although motivated by electrolyte films, the framework is general and applies broadly to confined, evaporating, deliquescent and coating films. By integrating deterministic and stochastic mechanisms within a single structure, this work provides a coherent basis for interpreting thin-film behavior under geometric asymmetry and offers a unifying perspective on inclination-driven effects across surface-physics contexts. It also defines clear directions for future extensions, including three-dimensional geometries, heterogeneous substrates and the coupling to fully resolved reactive models under intermittent wetting.

The aim of this work is to establish a unified and physically transparent theoretical structure rather than to provide fully resolved analytical or numerical solutions. The governing equations derived here enable such analyses, whether asymptotic treatments of specific drainage regimes or full numerical simulations, but these fall outside the scope of the present leading-order, system-independent framework. Future work may exploit the same formulation to obtain explicit solutions for targeted regimes or to quantify inclination effects in specific material systems.

Author Contributions: Conceptualization, H.C.V., M.G.M. and R.O.; methodology, H.C.V.; software, H.C.V.; validation, H.C.V., M.G.M. and R.O.; formal analysis, H.C.V.; investigation, H.C.V.; resources, R.O.; data curation, H.C.V.; writing—original draft preparation, H.C.V.; writing—review and editing, H.C.V., M.G.M. and R.O.; visualization, H.C.V.; supervision, R.O.; project administration, H.C.V. and R.O. All authors have read and agreed to the published version of the manuscript.

Funding: This research received no external funding.

Data Availability Statement: No new data were created or analyzed in this study.

Conflicts of Interest: The authors declare no conflicts of interest.

Abbreviations

The following abbreviations are used in this manuscript:

Bo	Bond number
Pe	Péclet number
Da	Damköhler number
EDL	Electric double layer
PDE	Partial differential equation

References

1. de Gennes, P.-G. (1985). *Wetting: Statics and dynamics*. *Reviews of Modern Physics, 57*(3), 827–863. https://doi.org/10.1103/RevModPhys.57.827
2. Snoeijer, J. H., & Andreotti, B. (2013). *Moving contact lines: Scales, regimes, and dynamical transitions*. *Annual Review of Fluid Mechanics, 45*(1), 269–292. https://doi.org/10.1146/annurev-fluid-011212-140734
3. Oron, A., Davis, S. H., & Bankoff, S. G. (1997). *Long-scale evolution of thin liquid films*. *Reviews of Modern Physics, 69*(3), 931–980. https://doi.org/10.1103/RevModPhys.69.931
4. Craster, R. V., & Matar, O. K. (2009). *Dynamics and stability of thin liquid films*. *Reviews of Modern Physics, 81*(3), 1131–1198. https://doi.org/10.1103/RevModPhys.81.1131
5. Starov, V. M., Velarde, M. G., & Radke, C. J. (2007). *Wetting and spreading dynamics*. CRC Press.
6. Derjaguin, B. V., Churaev, N. V., & Muller, V. M. (1987). *Surface forces*. Springer.

 doi:10.20944/preprints202603.2106.v1

7. Seemann, R., Herminghaus, S., & Jacobs, K. (2001). *Dewetting patterns and molecular forces: A reconciliation*. *Physical Review Letters, 86*(24), 5534–5537. https://doi.org/10.1103/PhysRevLett.86.5534
8. Thiele, U., Velarde, M. G., & Neuffer, K. (2001). *Dewetting: Film rupture by nucleation in the spinodal regime*. *Physical Review Letters, 87*(1), 016104. https://doi.org/10.1103/PhysRevLett.87.016104
9. Vrij, A. (1966). Possible mechanism for the spontaneous rupture of thin, free liquid films. Discussions of the Faraday Society, 42, 23–33. https://doi.org/10.1039/DF9664200023
10. Cook, B. P., Bertozzi, A. L., & Hosoi, A. E. (2008). *Shock solutions for particle-laden thin films*. *SIAM Journal on Applied Mathematics, 68*(3), 760–783. https://doi.org/10.1137/060677811
11. Bonn, D., Eggers, J., Indekeu, J., Meunier, J., & Rolley, E. (2009). *Wetting and spreading*. *Reviews of Modern Physics, 81*(2), 739–805. https://doi.org/10.1103/RevModPhys.81.739
12. Santana, J. J., Cano, V., Vasconcelos, H. C., & Souto, R. M. (2020). The influence of test-panel orientation and exposure angle on the corrosion rate of carbon steel: Mathematical modelling. Metals, 10(2), 196. https://doi.org/10.3390/met10020196
13. Chatzigiannakis, E., Jaensson, N., & Vermant, J. (2021). Thin liquid films: Where hydrodynamics, capillarity, surface stresses and intermolecular forces meet. Current Opinion in Colloid & Interface Science, 53, 101441. https://doi.org/10.1016/j.cocis.2021.101441
14. Rednikov, A., & Colinet, P. (2013). *Singularity-free description of moving contact lines for volatile liquids*. *Physical Review E, 87*(1), 010401(R). https://doi.org/10.1103/PhysRevE.87.010401
15. Zheng, Z., & Stone, H. A. (2022). *Spreading of complex fluids with a soft blade*. *Physical Review Fluids, 7*(8), 084002. https://doi.org/10.1103/PhysRevFluids.7.084002
16. Kumawat, T. C. (2024). Thin film flow inside a uniformly heated/cooled inclined rotating cylinder. Physics of Fluids, 36(4), 042103. https://doi.org/10.1063/5.0201250
17. Israelachvili, J. N., & Adams, G. E. (1978). Measurement of forces between two mica surfaces in aqueous electrolyte solutions in the range 0–100 nm. Journal of the Chemical Society, Faraday Transactions 1, 74(4), 975–1001. https://doi.org/10.1039/f19787400975
18. Oron, A., & Bankoff, S. G. (1999). Dewetting of a heated surface by an evaporating liquid film under conjoining/disjoining pressures. Journal of Colloid and Interface Science, 218(1), 152–166. https://doi.org/10.1006/jcis.1999.6390
19. Ajaev, V. S. (2005). Spreading of thin volatile liquid droplets on uniformly heated surfaces. Journal of Fluid Mechanics, 528, 279–296.
20. Cazabat, A.-M., & Guéna, G. (2010). *Evaporation of macroscopic sessile droplets*. *Soft Matter, 6*(12), 2591–2612. https://doi.org/10.1039/B924477H
21. Harvey, A. H. (2023). Improved and always improving—Reference formulations for thermophysical properties of water. *Journal of Physical and Chemical Reference Data, 52*(1), 011501.
22. Spiesz, P., Ballari, M. M., & Brouwers, H. J. H. (2012). RCM: A new model accounting for the non-linear chloride binding isotherm and the non-equilibrium conditions between the free- and bound-chloride concentrations. *Construction and Building Materials, 27*(1), 293–304. https://doi.org/10.1016/j.conbuildmat.2011.07.045